Journal of Technological Sciences Volume 1 [June 2023]

مجلة العلوم التكنولوجية
العدد الأول يونيه ٢٠٢٣

Load Frequency Control Using FOPID Controller for Multi-Source Power Systems

Nessma M. Ahmed [1], Mohamed Ebeed [2], Khairy Sayed [2], Alaa A. Mahmoud [1]*

1Elect. Dep., Faculty of Technology and Education, Sohag University, Sohag, Egypt
2Department of Electrical Engineering, Faculty of Engineering, sohag University, sohag, Egypt

ABSTRACT

Due to the constant integration of renewable energy sources (RESs) into the power grid and the variety of power systems with the continual increase in power demand in recent years, the management and control of the modern power system has grown complex and demanding. Load frequency control (LFC) can be used to solve a variety of difficulties, such as when a generating unit is quickly unplugged by protection equipment or when a heavy load is suddenly connected or disconnected. When the real power balance is affected by disturbances, the frequency deviates from the nominal value. The LFC oversees load balancing and restoring the natural frequency to its original state. The fractional-order proportional-integral-derivative (FOPID) controller for load frequency management was suggested in this article. The particle swarm optimization (PSO) approach is used to improve the gains for the FOPID controller to offer automatic LFC of the multi-source electricity system. When the FOPID controller's results are compared to the PID and PI controllers, the FOPID controller surpasses both. In terms of peak transient deviation and settling time, the MATLAB/Simulink findings show that the recommended controller has the best dynamic response of all the other controllers tested.

Keywords: FOPID Controller, PSO, LFC, RES.

1. INTRODUCTION

Due to the constant penetration of RESs integrated into the power grid and the structural variation of the electricity system with a continued escalation of power demand in recent years, the management and control of the modern electricity system has grown complex and demanding. Because of the depletion of fossil resources, environmental damage, and policy use, interest in renewable energy sources has grown. One of the most significant benefits of RESs is that they are available in almost every country[1], [2]. The concept of microgrid has grown in popularity as the use of renewable energy sources has increased. Small generators and loads are interconnected in microgrids, and the microgrid can operate standalone or in grid-connected mode, depending on the operational properties of the main grid. Microgrids provide high power supply dependability and operational efficiency while lowering transmission costs and losses. As a result, it appears that the quantity and variety of microgrid components can be expanded nowadays. [1], [3].

Solar and wind generators are examples of environmentally friendly acceptable RESs., but their output power fluctuation can cause excessive voltage and frequency deviations in the Electricity grid [4], [5]. The unpredictability and irregularity of these sources' production characteristics can sometimes result in power outages. energy storage systems such as batteries, and fuel cells are commonly used to improve system achievement and stability. When the demand for electricity exceeds the supply, these EBSSs generate electricity and store it when the supply exceeds the demand.[6]. The batteries in electric vehicles can help to improve the balance between load requests and power-generating systems. EV integrators are used to manage electric car owners' unpredictable behavior and to increase EV involvement in the ancillary services industry. Aggregators can create time-varying delays in load frequency control (LFC) schemes [7]. When developing the LFC controller, the impacts of these delays must be considered. Because the controller's efficacy is governed by its parameters, these parameters

Co-Author; Alaa A. Mahmoud: Alaa-Abd-El_samee@techedu.sohag.edu.eg
Received [1 Jan 2023 Accepted [13 March 2023]
Manuscript ID [JTS-2023-005]

should be designed so that the LFC system works as planned even when the delay varies over time [8].

The main responsibilities of the LFC are summarized as follows:

1. The system must be kept under control after an abrupt load disruption or any other disturbance.
2. The settling time, undershoot and overshoot of frequency and tie-line power variations should be decreased to maximize the system stability margin.
3. The area control error (ACE) must be reduced as much as feasible after a step load perturbation (SLP).
4. At a steady state, each area should be able to handle its own load.
5. Areas in need of power can partner with one another in a temporary state.

Microgrid control models have gained popularity in recent years due to the dynamic interplay of various energy providers and storage systems. Many LFC control methods have been devised to ensure better disturbance rejection and quality over a wider range of frequencies while yet allowing for frequency transients, overshoots, and system robustness.

In multi-source electric power production systems, the fractional-order proportional-integral (FOPI) – fractional-order proportional derivative (FOPD) cascade controller for LFC has been introduced [9]. To alter all console gain and fractal order properties at once, the Dragonfly Search Algorithm (DSA) is utilized. PHEVs have been explored by multiple writers for planned load frequency control (LFC) research with various controllers throughout the previous decade [10]–[12]. In [13] , the FOPID controller parameters are optimized using the elephant herding optimization (EHO) method. [4] illustrates how to regulate the load frequency in a stand-alone micro-grid using the proposed method, which uses a fuzzy way to circumvent the constant parameters of a traditional PID controller. The parameters of the FOPID controller in the LFC of the micro-grid were accessed using a swarm-based multi-objective (MOGO) algorithm in [14]. To increase the performance of the FOPID controller in obtaining system parameters, a Learning and Teaching Based Optimization (TLBO) technique is presented in [15], [16]. To achieve the controlling aims, the optimum FOPID controller is utilized as an LFC system in [17], and the salp swarm algorithm (SSA) is used to design the supplied controller coefficients and subscription ratio of each EVs aggregator. The epsilon multi-objective genetic (ε-MOG) algorithm is used to optimize the parameters of the recommended controllers in [18]. Despite the existence of other better control systems, PID control is the most extensively used control method in the industry owing to its stability, ease of construction, wide applicability, and satisfaction of use in both digital and analog platforms. As a result, the objective is to improve the characteristics of a typical PID controller to produce a new controller. The FOPID controller, an enhanced variant of the traditional PID controller that employs fractional calculus, has been the subject of scientific research [19]–[21]. This paper presents a new implementation of LFC control for a multi-source microgrid system using the FOPID controller.

The remainder of the article is organized as follows: The modeling of the component of the microgrid multi-source microgrid is discussed in Section 2. Section 3 describes the layouts of the analyzed system. Section 4 explains the suggested FOPID controller. Section 5 delves into the PSO algorithm in depth. Section 6 displays the simulation findings. Finally, the important findings and conclusions are provided in section 7.

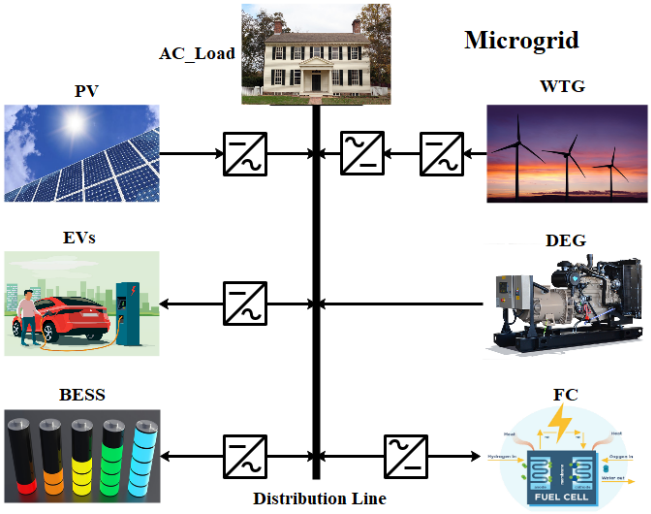

Fig. 1: The schematic model of the Proposed system

2. DESCRIPTION OF THE PROPOSED MULTI-SOURCE SYSTEM

This suggested system contains a solar power (PV), wind turbine generator (WTG), diesel energy generator (DEG), electric vehicles (EVs), fuel cells (FCs), battery energy storage system (BESS), and a load model, as shown schematically in Fig 1 and 2. In this analysis, both WTG and PV power are considered uncontrollable power sources (as disturbances). These sources must limit their MPPT output power depending on frequency variations

if they participate in frequency regulation, diminishing the benefits of renewable energy use.

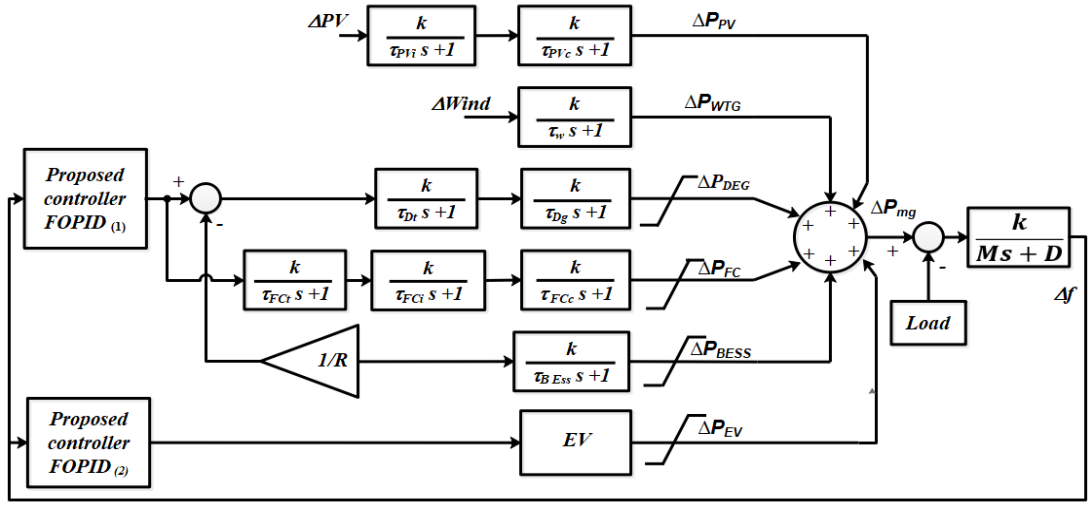

Fig. 2: Block diagram of the studied microgrid

DEGs, FCs, and EVs are used to control the frequency in this proposed. The FOPID controller will balance residual power between DEGs, FCs, and EVs based on renewable power output and load requirements. The equation for the microgrid power balance is as follows:

$$\Delta P_{Load} = \Delta P_{PV} + \Delta P_{WTG} + \Delta P_{FC} + \Delta P_{DEG} + \Delta P_{EV} + \Delta P_{BESS} \quad (1)$$

Based on generation and load, the frequency deviation (Δf) in a microgrid can be stated as:

$$\Delta f = \frac{1}{Ms + D}(\Delta P_{PV} + \Delta P_{WTG} + \Delta P_{FC} + \Delta P_{DEG} + \Delta P_{EV} - \Delta P_{BESS} - \Delta P_{Load} - \alpha\Delta f) \quad (2)$$

In the literature, many architectures for load-frequency control in microgrids that are mostly independent of the grid have been presented. Fig. 2 depicts the load-frequency control structure presented in this paper. The following mathematical model can be used to express the suggested system.

The change in solar photovoltaic (ΔPPV) output power can be expressed as

$$\frac{\Delta P_{PV}}{\Delta G_{PV}} = \frac{k}{\tau_{PV_i}s + 1} * \frac{k}{\tau_{PV_c}s + 1} \quad (3)$$

The change in wind turbine sources output power (ΔPWTG) can be expressed as

$$\frac{\Delta P_{WTG}}{\Delta V_{Wind}} = \frac{1}{\tau_{WTG}\,s + 1} \quad (4)$$

The difference in (ΔPDEG) diesel-energy generator power can be expressed as

$$\frac{\Delta P_{DEG}}{Uc} = \frac{k}{\tau_{DEG_g}s + 1} * \frac{k}{\tau_{DEG_t}s + 1} \quad (5)$$

The change in the output power of a battery energy storage system (ΔPBESS) is expressed as

$$\frac{\Delta P_{BES}}{\Delta f} = \frac{1}{\tau_{BESS}S + 1} \quad (6)$$

A fuel cell's (ΔPFC) output power change can be written as

$$\frac{\Delta P_{FC}}{Uc} = \frac{1}{\tau_{FC}S + 1} \quad (7)$$

where τWTG and τPV denotes the conversion time constants of wind and solar systems respectively. where τFESS, and τFC denotes the conversion time constants of battery, and fuel cells.

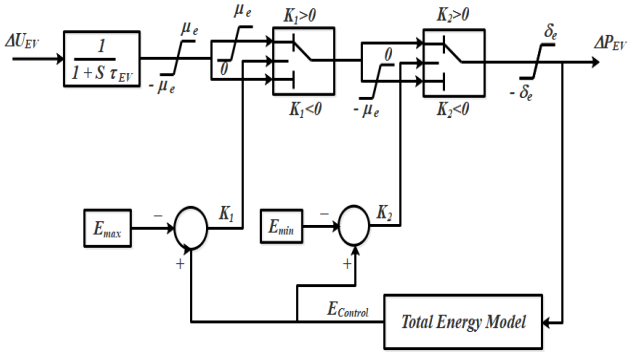

Fig. 3: The transfer function model of EV model for LFC

The time constant of EV is τEV, the LFC signal transmitted to EV is ΔuE, the inverter capacity limitations are ±μe, and the power ramp rate limits are ±δe in Fig. 3. The differences between the EV battery's limiting energy

and current energy are K1 and K2, respectively. The complex frequency is s, and the formula is s = δ+ jw. E is the EV battery's current energy. The EV battery's min and max controlled energy, respectively, are Emax and Emin. K1 = E-Emax and K2 = E-Emin can be used to compute them. Finally, the charging or discharging power is referred to as PE. ΔPE = 0 indicates that the EV is in the idle state, ΔPE > 0 indicates that the EV is discharging, and ΔPE < 0 indicates that the EV is charging. Only within the range of e can the EV be charged and discharged. If the EV's energy surpasses the top limit i.e., Emax, the EV can only be discharged within the -μe range. In addition, if the EV's energy is below the lower limit (i.e., Emin), it can only be charged within the range of -μe ~ 0 [22], [23].

The initial state of charge (SOC) of all controlled EVs is 85 percent in Fig 4. The number of controlled EVs and the EV customers' convenience, as indicated by the set SOC, might restrict the reaction to the LFC signal. $E_{control\_in}$ is the energy increase caused by EVs changing from a charging to a controlled state. E_{LFC} is the energy equivalent to the LFC signal. The value is derived from the integral of the control-in rate ($R_{control\_in}$), where E_o is the beginning energy, E_{plug_out} is the energy loss due to plug-out EVs, $N_{control\_in}$ is the number of controllable EVs, and No is the number of initial controllable EVs. Based on charging and discharging characteristics, literature [7], [23] contains specifics on a similar EV model, including battery and charger.

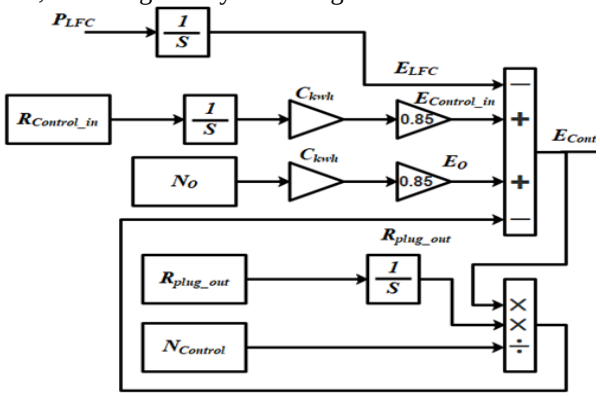

Fig. 4: Total energy model.

The test system parameters are given in Table 1

TABLE 1. MICROGRID SIMULATION PARAMETERS

Parameter	Value	Parameter	Value
M	0.1667	τ_{PV_i}	0.04
D (puMW/Hz)	0.015	τ_{PV_C}	0.004
$\tau_{EV} = K$	1	τ_{D_t}	0.4
δe (Pu.MW/s)	0.05	τ_{D_g}	0.08
μe (pu.MW)	0.015	τ_{BESS}	0.1
$Emax.$ (pu.MWh)	0.90	τ_{FC_t}	0.26
$Emin.$ (pu.MWh)	0.80	τ_{FC_i}	0.04
τ_{wTG}	1.5	τ_{FC_c}	0.004

3. CONTROLLER STRUCTURAL DESIGN

The suggested controller and optimization method are detailed in this article.

3.1 PID controller

Fig. 5 depicts a classical PID controller. The most often utilized controller in practically all industrial operations [24], [25]. Because of its simple structure and toughness, it may give good control performance. PID is the simplest controller to understand. One of its most important features is to reduce the rise time using the proportional control device and using an integrated model, the steady-state error can be avoided. A PID controller is a type of control technique that is commonly employed in industrial processes. The "three terms" controller is a common PID controller structure that can be given using Eq. (9), and it has the transfer function given by Eq. (10) [26], [27].

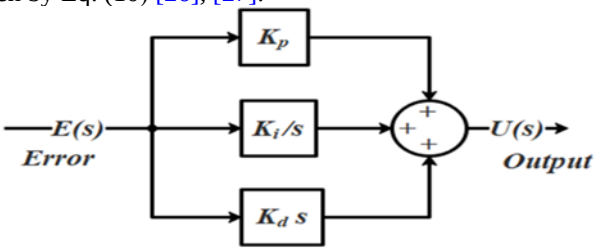

Fig. 5: Structure of conventional PID controller

$$u(t) = K_P\, e(t) + K_i \int_0^t e(t)\, dt + K_d \frac{de(t)}{dt} \quad (9)$$

$$G(s) = K_P + \frac{K_i}{s} + K_d s \quad (10)$$

3.2 Fractional Order PID Controller

FOPID controllers, unlike classical PID controllers, were born from the idea of combining fractional calculus theory with the PID controller. A non-integer-order controller with two additional degrees of opportunity is the FOPID controller. a new PID controller family member that has grabbed the curiosity of many controller designers [28], [29].

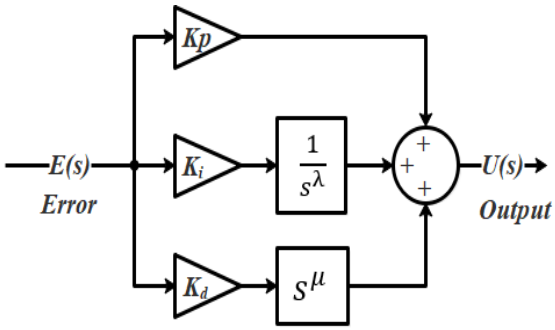

Fig. 6: Structure of fractional order PID controller.

The integral and derivative term orders are detected by λ and μ, respectively. As demonstrated in Fig. 6, the classic PID controller is the true beginning of the FOPID controller. The FOPID behaves like a PID controller when λ and μ is equal to one [27], [30]. The additional tuning coefficients and in the case of a partial-order PID controller enable more latitude in the construction of a control system λ and μ thus provide more scope for modifying the system dynamics. Eqs. (11) and (12), respectively, represent the FOPID controller transfer function [28], [29], [31]:

$$u(t) = K_P\, e(t) + K_i\, D^{-\lambda}\, e(t) + K_d\, D^{\mu}\, e(t) \quad (11)$$

$$G(s) = K_P + \frac{K_i}{s^{\lambda}} + K_d s^{\mu} \quad (12)$$

4. PSO ALGORITHM

Particle swarm optimization (PSO) is a stochastic population-based optimization method developed by James Kennedy and Russell Eberhart in 1995. It was developed by research on the social behavior of birds and fish education. Each particle in the swarm represents the unknown parameters of the g oal function to be improved. The swarm consists of N particles traveling in a D-dimensional search space. When a particle is produced, it is given a random position and velocity. In this technique, each bird is represented as a particle, and the swarm is made up of all the particles. Each particle's position and velocity are represented by two vectors, Xi and VI. Each particle's position at any given time is seen as a solution to the problem at hand. The particles then wander throughout the search area, changing their speed and position to find the optimal response at all times (best location). The following vectors indicate the position and velocity of the particle I in the physical search space D dimensions [32], [33]:

$$\left.\begin{aligned} X_i &= [x_i^1, x_i^2, x_i^3, \dots\dots, x_i^d] \\ V_i &= [v_i^1, v_i^2, v_i^3, \dots\dots\dots, v_i^d] \end{aligned}\right\} \quad (13)$$

The optimum location for a particle is the one that gives that particle the lowest objective value (J).

Let $P_{best_i} = [P_{best_i^1}, P_{best_i^2}, P_{best_i^3} \dots P_{best_i^d}]$ be the best position in the swarm population that yields the best fitness value for the ith particle, and $G_{best_i} = [G_{best_i^1}, G_{best_i^2}, G_{best_i^3} \dots G_{best_i^d}]$ be the global best position. The following equation is used by the PSO algorithm to update its velocity and location [34].

$$V_i^{d(k+1)} = W\left(V_i^{d(k)}\right) + c_1(rand_1)\left(Pbest_i^{d(k)} - X_i^{d(k)}\right) + c_2(rand_2)\left(Gbest_i^{d(k)} - X_i^{d(k)}\right) \quad (14)$$

$$X_i^{d(k+1)} = X_i^{d(k)} + V_i^{d(k+1)} \quad (15)$$

The learning variables c_1=2 and c_2=2 govern the proportionate effect of the cognitive and social components on updating the particle's location and velocity. The two random numbers $rand_1$ and $rand_2$ are picked from the range [0, 1]. $V_i^{d(k)}$ and $X_i^{d(k)}$ are the velocity and location of the ith particle in the dth dimension at the kth iteration, respectively. $Gbest_i^{d(k)}$ is the global best of ith particle in dth dimension at kth iteration, whereas $Pbest_i^{d(k)}$ is the personal best of ith particle in dth dimension at kth iteration? W is the inertia weight parameter, which controls the exploration and utilization of the search space. The following equation is used to set the weight parameter W [35]:

$$W = W_{max} - \left(\frac{W_{max} - W_{max}}{Iter_{max}}\right) * Iter \quad (16)$$

W_{max} and W_{min} are the beginning and ultimate weights, respectively. The current number of iterations is Iter, and the maximum number of iterations is $Iter_{max}$. The speed of the particle is limited to a specified dynamic range (V_{max},V_{min}). The highest particle velocity allowed is V_{max}. When the particle hits Vmax, its velocity is lowered to V_{max}. It's worth mentioning that if this parameter's value is set high, the particle may be shifted beyond what is

sensible. Particle mobility will be hindered if it's too low, and the best option may be neglected.

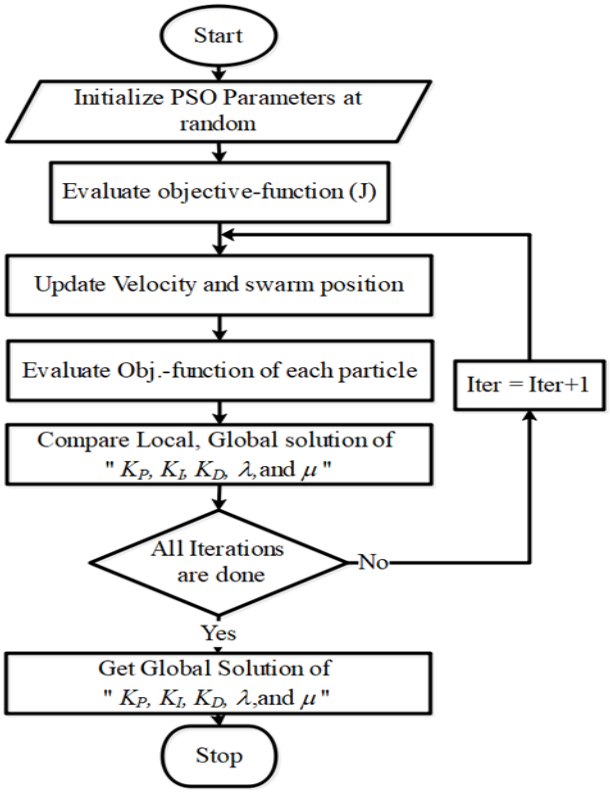

Fig. 7: Flowchart of PSO algorithm

PSO algorithms may be summarized as follows:

Step 1: In the problem space, create a inhabitance of particles with random locations and velocities on D-dimensions.

Step 2: For each particle, determine the D-dimensional optimization fitness function that is necessary.

Step 3: Assess the particle's fitness in comparison to its previous best location. Set the best prior location equal to the current value if the current value is better, and pi = the current point xi in D dimensional space.

Step 4: To the variable g, add the index of the particle in the neighborhood with the best fitness thus far.

Using Eqs. (14) and (15), change the particle's velocity and location (15).

Return to step 2 until all of the iterations have been completed or a condition has been met.

Fig. 7 depicts the flowchart of this method as follows:

5. SIMULATION RESULTS

The test system was implemented as a Simulink model using the MATLAB (R2018b) software on an i7-3537 CPU@ 2.00 GHz with 8 GB RAM. Also, the proposed algorithm was implemented using MATLAB. Furthermore, the optimization technique PSO was also implemented using MATLAB. the algorithm with the MATLAB Simulink model of the test system to obtain a comparative performance evaluation. The effectiveness of the proposed controller was evaluated under dynamic system operating settings using different case studies. The parameters of the FOPID controller were optimized by minimizing the ITAE using the optimization technique. The PSO optimization approach was used to determine the FOPID controller's optimal parameters. To elucidate the efficacy of the suggested controller, we considered three cases, which are described below. Using the PSO technique, the parameters of the controller are derived by minimizing the ITAE of the frequency deviation (16).

$$ITAE = \int_0^{t_{sim}} t\,|\Delta f|\,dt \qquad (16)$$

5.1 Step Load Change of case (1)

A PL loading disturbance of 3% pu is provided at time t = 1s to test the efficiency of the suggested FOPID with a non-constant progressive change in wind and PV, as shown in Fig. 8. The simulation is run on the multi-source model that has been suggested. Fig. 9 shows the frequency responses of the microgrid examined using the PI, PID, and FOPID controllers. The recommended controller reduces frequency oscillations faster than the PI and PID controllers, as seen in Fig. 9. Table 2 also lists the dynamic coefficients of the investigated controllers. As a result, the suggested controller outperforms existing controllers in terms of frequency performance.

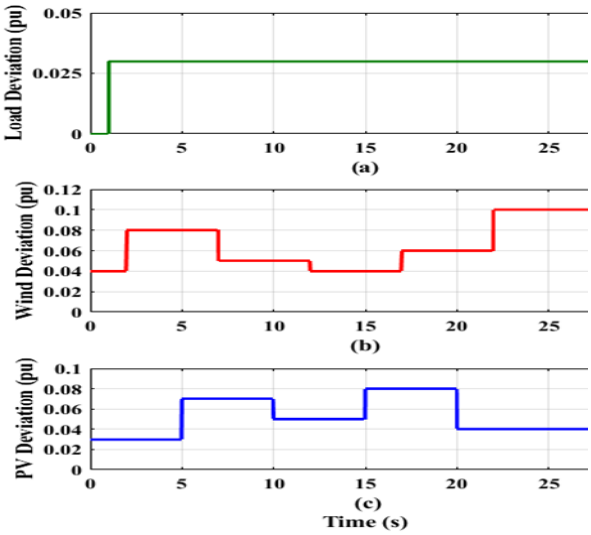

Fig. 8: Multi-Source Microgrid disturbances of case 1 (a) The pattern of considered load disturbance. (b) Wind input power. (c) PV input power.

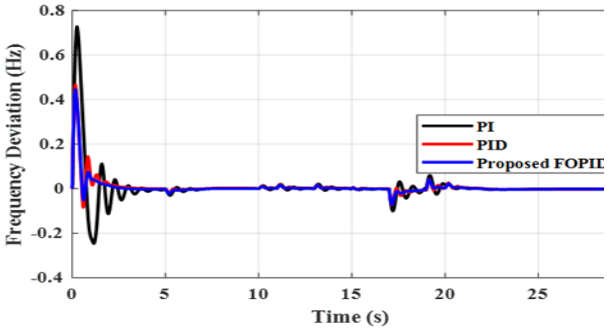

Fig. 9 Frequency responses generated by case (1)

TABLE 2 OPTIMIZED SYSTEM PARAMETERS VALUES OF CASE (1)

Controller / Parameters		PI	PID	FOPID
(1)	Kp_1	1.6512	2.0000	1.5559
	Ki_1	2.0000	2.0000	2.0000
	Kd_1	--	0.2082	0.5685
	λ_1	--	--	0.9287
	μ_1	--	--	0.6009
(2)	Kp_2	0.8215	0.3665	0.7365
	Ki_2	1.1560	1.0250	1.2539
	Kd_2	--	0.7968	1.0892
	λ_2	--	--	1.0697
	μ_2	--	--	0.9262
The objective Function		1.5677	0.95902	0.94692

5.2 Random Load Change of case (2)

To further test the effectiveness of the suggested control strategy, a disturbance like that seen in Fig. 10a is introduced to the Multi-Source Microgrid. Variations in wind power ΔPwind and solar PV system ΔPPV are also studied to illustrate the performance of the proposed controllers, as illustrated in Fig. 10b and c. Fig. 11 depicts the results.

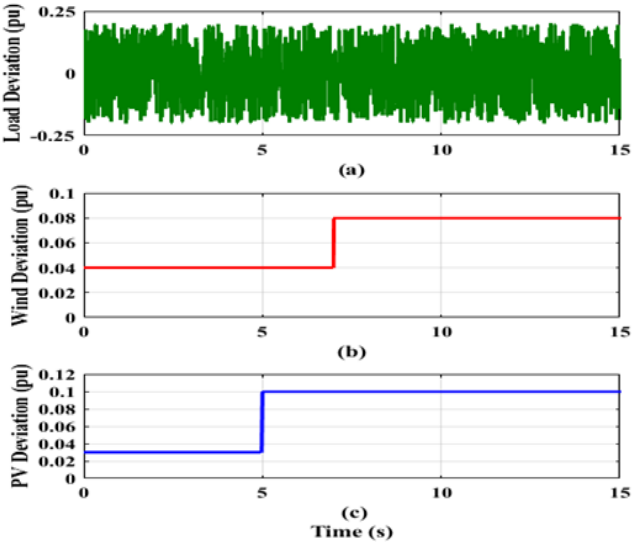

Fig. 10 Multi-Source Microgrid disturbances of case 2(a) Random load deviation pattern. (b) Wind input power. (c) PV input power

The suggested controller, obviously, has a smaller fluctuation amplitude than the others. Table 2 also lists the dynamic coefficients of the investigated controllers. Although all three controllers return the Δf to its operating value, the optimized FOPID outperforms the other two controllers in terms of overshoot, settling time, and frequency minimization, as seen in this case (2).

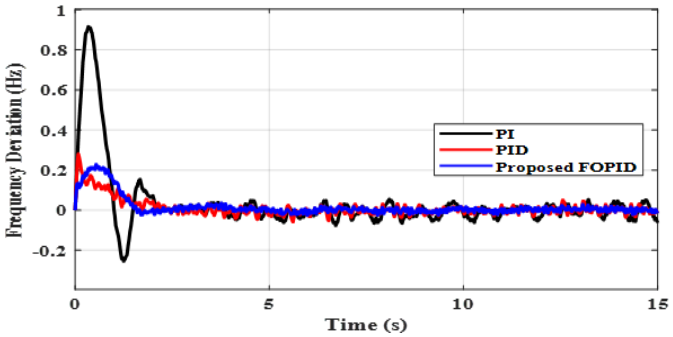

Fig. 11 Frequency responses generated by case (2)

5.3 A Sequence of Step Load Changes of the case (3)

A succession of step load modifications is applied to Multi-Source Microgrid, as shown in Fig. 12a. Fig. 12 b and c shows the variances in WTG and PV input powers for this scenario. Fig. 13 shows the frequency responses of a Multi-Source Microgrid using standard PI, PID, and suggested FOPID controllers. Moreover, Table 2 shows the dynamic coefficients of the studied controllers. The suggested FOPID controller is more efficient than typical PI, PID controllers at dampening swings and lowering their amplitude, as seen in Fig. 13.

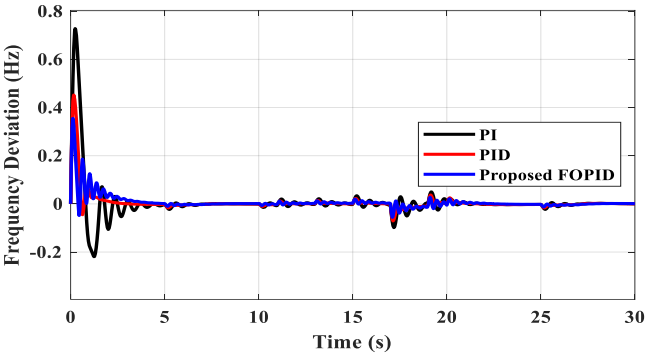

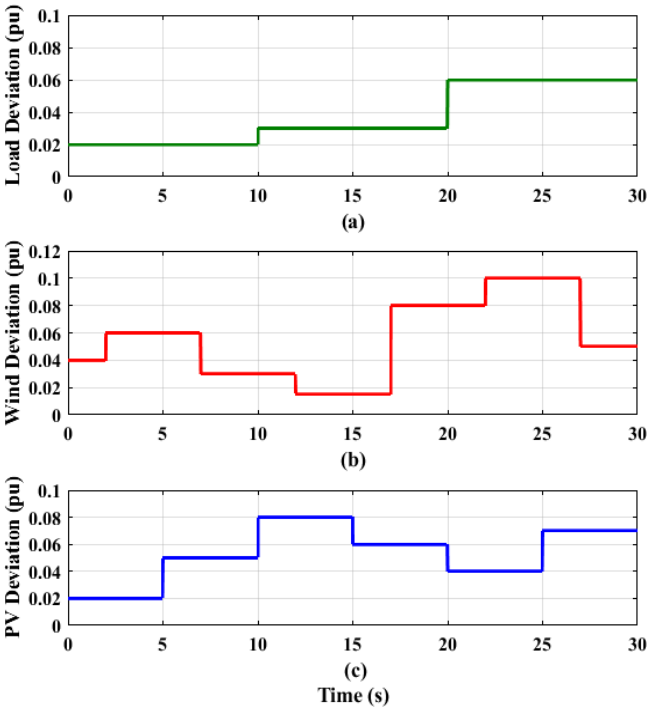

Fig. 12 Multi-Source Microgrid disturbances of case 1 (a) The pattern of considered load disturbance. (b) Wind input power. (c) PV input power.

Fig. 13 Frequency responses generated by case (3)

6. CONCLUSIONS

The main points that have been presented by this paper can be concluded as follows:

The proposed FOPID controller has been applied on the microgrid that includes WT/ PV/ Fuel Cell / Diesel/ PEV for tackling the LFC problem.

The system's performance was evaluated with the suggested FOPID controller implemented, and the results were compared to those obtained with application PID and PI controllers.

The PSO method was used to determine the best parameters for the proposed controller.

The study makes use of a step change in the load, the generated power of the PV unit, and the wind speed. In addition, the system's performance is assessed in the presence of random fluctuations in loads, PV unit produced power and wind speed.

The system performance of the microgrid for LFC is enhanced efficiently by the implementation of the

suggested FOPID controller compared with PI and PID controllers.

REFERENCES

[1] R. Mohamed, M. Helaimi, R. Taleb, H. A. Gabbar, and A. M. Othman, "Frequency control of microgrid system based renewable generation using fractional PID controller," vol. 19, no. 2, pp. 745–755, 2020, doi: 10.11591/ijeecs.v19.i2.pp745-755.

[2] B. Mohammadi-ivatloo, "Provision of Frequency Stability of an Islanded Microgrid Cascade Controller," *Energies*, 2021.

[3] R. K. Khadanga, S. Padhy, S. Panda, and A. Kumar, "Design and Analysis of Tilt Integral Derivative Controller for Frequency Control in an Islanded Microgrid: A Novel Hybrid Dragonfly and Pattern Search Algorithm Approach," *Arab. J. Sci. Eng.*, vol. 43, no. 6, pp. 3103–3114, 2018, doi: 10.1007/s13369-018-3151-0.

[4] A. Naderipour, Z. Abdul-Malek, I. F. Davoodkhani, H. Kamyab, and R. R. Ali, "Load-frequency control in an islanded microgrid PV/WT/FC/ESS using an optimal self-tuning fractional-order fuzzy controller," *Environ. Sci. Pollut. Res.*, 2021, doi: 10.1007/s11356-021-14799-1.

[5] A. H. Yakout, H. Kotb, H. M. Hasanien, and K. M. Aboras, "Optimal Fuzzy PIDF Load Frequency Controller for Hybrid Microgrid System Using Marine Predator Algorithm," *IEEE Access*, vol. 9, pp. 54220–54232, 2021, doi: 10.1109/ACCESS.2021.3070076.

[6] P. Sanki, S. Mazumder, M. Basu, P. S. Pal, and D. Das, "Moth Flame Optimization Based Fuzzy-PID Controller for Power–Frequency Balance of an Islanded Microgrid," *J. Inst. Eng. Ser. B*, vol. 102, no. 5, pp. 997–1006, 2021, doi: 10.1007/s40031-021-00607-4.

[7] M. U. Jan, A. Xin, H. U. Rehman, M. A. Abdelbaky, S. Iqbal, and M. Aurangzeb, "Frequency Regulation of an Isolated Microgrid with Electric Vehicles and Energy Storage System Integration Using Adaptive and Model Predictive Controllers," *IEEE Access*, vol. 9, no. January, pp. 14958–14970, 2021, doi: 10.1109/ACCESS.2021.3052797.

[8] A. S. Mohammed, "Fractional Order PID Controller for Minimizing Frequency Deviation in a Single and Multi-area Power System with Physical Constraints," vol. 3, no. 1, pp. 32–47, 2022, doi: 10.18196/jrc.31148.

[9] E. Çelik, "Design of new fractional order PI – fractional order PD cascade controller through dragonfly search algorithm for advanced load frequency control of power systems," *Soft Comput.*, vol. 25, no. 2, pp. 1193–1217, 2021, doi: 10.1007/s00500-020-05215-w.

[10] M. Khooban, T. Niknam, and M. Shasadeghi, "Load Frequency Control in Microgrids Based on a Stochastic Non-Integer Controller," vol. 3029, no. c, pp. 1–9, 2017, doi: 10.1109/TSTE.2017.2763607.

[11] H. Jia *et al.*, "Coordinated control for EV aggregators and power plants in frequency regulation considering time-varying delays," *Appl. Energy*, vol. 210, no. 2018, pp. 1363–1376, 2020, doi: 10.1016/j.apenergy.2017.05.174.

[12] V. Kleftakis, D. Lagos, C. Papadimitriou, and N. D. Hatziargyriou, "Seamless Transition between Interconnected and Islanded Operation of DC Microgrids," *IEEE Trans. Smart Grid*, vol. 10, no. 1, pp. 248–256, 2019, doi: 10.1109/TSG.2017.2737595.

[13] D. K. Sambariya and O. Nagar, "Optimal Design and Comparative Analysis of FOPID Controller for Three Area LFC Tuned Using EHO and GCMBO Algorithms," vol. 5, no. 1, pp. 6–14, 2018, doi: 10.12691/iteces-5-1-2.

[14] A. Tabak, "Fractional order frequency control of microgrid consisting of renewable energy sources based on multi-objective grasshopper optimization algorithm," vol. 44, no. 42, pp. 378–392, 2022, doi: 10.1177/01423312211034660.

[15] J. Bhookya, "Fractional Order PID Controller Design for Multivariable Systems using TLBO Abstract :," pp. 1–12, 2019, doi: 10.1515/cppm-2019-0061.

[16] A. Annamraju, "Robust frequency control in a renewable penetrated power system : an adaptive fractional order-fuzzy approach," 2019.

[17] F. Babaei, Z. B. Lashkari, A. Safari, M. Farrokhifar, and J. Salehi, "Salp swarm algorithm-based fractional-order PID controller for LFC systems in the presence of delayed EV aggregators," vol. 10, pp. 259–267, 2020, doi: 10.1049/iet-est.2019.0076.

[18] A. F. Abdel-gawad and A. Yona, "A Frequency Control Approach for Hybrid Power System Using Multi-Objective Optimization," pp. 1–22,

2017, doi: 10.3390/en10010080.

[19] J. Z. Shi, “A Fractional Order General Type-2 Fuzzy PID Controller Design Algorithm,” *IEEE Access*, vol. 8, pp. 52151–52172, 2020, doi: 10.1109/ACCESS.2020.2980686.

[20] X. Bao, D. Wang, and Y. Yang, “Fuzzy Fractional Order PI λ D μ Controller Design Based on Correction Projectile System,” vol. 9, no. 12, pp. 335–346, 2016.

[21] R. Lamba, S. K. Singla, and S. Sondhi, “Electric Power Components and Systems Design of Fractional Order PID Controller for Load Frequency Control in Perturbed Two Area Design of Fractional Order PID Controller for Load Frequency Control in Perturbed Two Area Interconnected System,” *Electr. Power Components Syst.*, vol. 0, no. 0, pp. 1–14, 2019, doi: 10.1080/15325008.2019.1660736.

[22] F. Babaei and A. Safari, “SCA based Fractional-Order PID Controller Considering Delayed EV Aggregators,” vol. 8, no. 1, pp. 75–85, 2020.

[23] S. Padhy, S. Panda, and S. Mahapatra, “A modified GWO technique based cascade PI-PD controller for AGC of power systems in presence of Plug in Electric Vehicles,” *Eng. Sci. Technol. an Int. J.*, vol. 20, no. 2, pp. 427–442, 2017, doi: 10.1016/j.jestch.2017.03.004.

[24] A. Idir, “Speed Control of DC Motor Using PID and FOPID Controllers Based on Differential Evolution and PSO,” vol. 11, no. 4, pp. 241–249, 2018, doi: 10.22266/ijies2018.0831.24.

[25] R. Ramjug-Ballgobin and C. Ramlukon, “A hybrid metaheuristic optimisation technique for load frequency control,” *SN Appl. Sci.*, vol. 3, no. 5, pp. 1–14, 2021, doi: 10.1007/s42452-021-04482-y.

[26] R. K. Khadanga, A. Kumar, and S. Panda, “A novel sine augmented scaled sine cosine algorithm for frequency control issues of a hybrid distributed two-area power system,” *Neural Comput. Appl.*, vol. 33, no. 19, pp. 12791–12804, 2021, doi: 10.1007/s00521-021-05923-w.

[27] E. D. Atsari, A. Halim, and Z. Nichols, “Design of a fractional order PID controller for electro hydraulic actuator,” vol. 4, 2021.

[28] C. Engineering, “Design of Fractional Order PID Controller Using Genetic Algorithm Optimization Technique for Nonlinear System Abstract :,” pp. 1–11, 2020, doi: 10.1515/cppm-2019-0072.

[29] Y. A. Ajmera and S. S. Sankeshwari, “Fractional order PID Controller : Design and Comparison with Conventional PID Controller for the Robust Control of DC Motor using Fuzzy SMC,” vol. 12, no. 4, pp. 47–54, 2017, doi: 10.9790/1676-1204024754.

[30] W. Aldawasir and S. Arabia, “Design and Performance Evaluation of Fuzzy Variable Fractional-Order [PI] λ D μ Controller for a Class of First-Order Delay-Time Systems *,” vol. 28, no. December, pp. 443–452, 2019, doi: 10.1155/2018/5478781.

[31] C. H. R. Kumar, “IMPLEMENTATION OF FRACTIONAL ORDER PID CONTROLLER FOR LFC,” vol. 5, no. 3, pp. 1225–1229, 2018.

[32] N. K. Bahgaat, M. I. E. Ahmed, M. Ahmed, M. Hassan, and F. Bendary, “Load Frequency Control Based on Evolutionary Techniques in Electrical Power,” no. April, 2016, doi: 10.1007/978-3-319-30340-6.

[33] S. Kumar, “Fractional order PID Controller design for Load Frequency Control in Parallel Control Structure,” *2019 54th Int. Univ. Power Eng. Conf.*, pp. 1–6, 2019.

[34] A. Djari, T. Bouden, and A. Boulkroune, “Design of fractional-order PID controller (FOPID) for a class of fractional-order MIMO systems using a particle swarm optimization (PSO) approach Design of Fractional-Order PID Controller (FOPID) for a Class of Fractional-Order MIMO Systems Using a Particle Swarm Optimization (PSO) Approach,” no. November 2016, 2013, doi: 10.1109/ICoSC.2013.6750985.

[35] M. R. Dastranj, M. Rouhani, and A. Hajipoor, “Design of Optimal Fractional Order PID Controller Using PSO Algorithm,” vol. 4, no. 3, pp. 429–432, 2012.

التحكم في تردد الحمل باستخدام وحدة التحكم FOPID لأنظمة الطاقة متعددة المصادر

الملخص:

نظرًا للدمج المستمر لمصادر الطاقة المتجددة **(RESs)** في شبكة الطاقة وتنوع أنظمة الطاقة مع الزيادة المستمرة في الطلب على الطاقة في السنوات الأخيرة ، فقد أصبحت إدارة نظام الطاقة الحديث والتحكم فيه أمرًا معقدًا ومتطلبًا. يمكن استخدام التحكم في تردد الحمل لحل مجموعة متنوعة من الصعوبات ، مثل عندما يتم فصل وحدة توليد بسرعة عن طريق معدات الحماية أو عند توصيل حمولة ثقيلة أو فصلها فجأة. عندما يتأثر توازن الطاقة الحقيقي بالاضطرابات ، ينحرف التردد عن القيمة الاسمية. يشرف التحكم في تردد الحمل على موازنة الحمل واستعادة التردد الطبيعي إلى حالته الأصلية. تم اقتراح وحدة تحكم المشتق النسبي المتكامل (FOPID) من أجل إدارة تردد الحمل في هذه المقالة. يتم استخدام نهج تحسين سرب الجسيمات (PSO) لتحسين المكاسب لوحدة التحكم FOPID لتقديم التحكم في تردد الحمل التلقائي لنظام الكهرباء متعدد المصادر. عندما تتم مقارنة نتائج وحدة تحكم FOPID بوحدات تحكم PID **و** PI ، فإن وحدة تحكم FOPID تتفوق على كليهما. من حيث ذروة الانحراف العابر ووقت الاستقرار ، تُظهر نتائج MATLAB / Simulink أن وحدة التحكم الموصى بها لديها أفضل استجابة ديناميكية لجميع وحدات التحكم الأخرى التي تم اختبارها.